VŠB – Technical University of Ostrava
Faculty of Electrical Engineering and Computer Science
Department of Computer Science

Analysis of the Sources of Brain Electrical Activity Obtained Via Independent Component Analysis

Analýza zdrojů elektrické aktivity v mozku získaných pomocí analýzy nezávislých komponent

2016 Elena Lavlinskaya

VŠB - Technical University of Ostrava
Faculty of Electrical Engineering and Computer Science
Department of Computer Science

Diploma Thesis Assignment

Student: **Bc. Elena Lavlinskaya**

Study Programme: N2647 Information and Communication Technology

Study Branch: 2612T025 Computer Science and Technology

Title: Analysis of the Sources of Brain Electrical Activity Obtained Via Independent Component Analysis
Analýza zdrojů elektrické aktivity v mozku získaných pomocí analyzy nezávislých komponent

The thesis language: English

Description:

The goal is to find whether using vector autoregressive model is feasible, when input signal is obtained by independent components methods.

1. Study the concept of autoregressive model, learn to generate autoregressive signal with given parameters.
2. Study methods of signal interaction analysis: Granger causality and directed coherence.
3. Find out whether independent components can have non-zero coherence.
4. Evaluate interaction of the brain electrical activity sources.

References:

[1] V.S. Ramachandran, The Tell-Tale Brain: A Neuroscientists's Quest for What Makes Us Human, W. W. Norton & Company, ISBN 978-0-393-07782-7
[2] Eva Möller, Bärbel Schack, Matthias Arnold, Herbert Witte, Instantaneous multivariate EEG coherence analysis by means of adaptive high-dimensional autoregressive models, Journal of neuroscience methods, vol. 105, pp. 143-158
[3] Wolfram Hesse, Eva Möller, Matthias Arnold, Bärbel Schack, The use of time-variant EEG Granger causality for inspecting directed interdependencies of neural assemblies, Journal of neuroscience methods, vol. 124, pp. 27-44
[4] Brain-Computer Interface Systems - Recent Progress and Future Prospects, book edited by: Reza Fazel-Rezai, InTech, ISBN 978-953-51-1134-4

Extent and terms of a thesis are specified in directions for its elaboration that are opened to the public on the web sites of the faculty.

Supervisor: **prof. RNDr. Václav Snášel, CSc.**

Date of issue: 01.09.2014

Date of submission: 29.04.2016

doc. Dr. Ing. Eduard Sojka
Head of Department

prof. RNDr. Václav Snášel, CSc.
Dean of Faculty

I hereby declare that this master's thesis was written by myself. I have quoted all the references I have drawn upon.

Ostrava, April 29th, 2016 .....

I'd like to thank my supervisor prof. RNDr. Václav Snášel, CSc. for his valuable time and knowledge on the subject. I'd also like to thank my thesis advisor prof. Alexandr Frolov and his fellow student Yaroslav Kerechanin for their time and patience. Without their help, this work would have never seen the light of day.

Abstract

This work shows existing methods for analysing electrical activity sources in the brain and for searching for functional connections among these sources. The work tries to answer the question of feasibility of looking for these connections among sources obtained by independent component analysis. Connections found between some sources in EEG records obtained on real subjects are presented.

Key Words: independent component analysis, EEG, vector autoregressive model, spectral coherence, partial directed coherence, Granger causality, sources of electrical brain activity

Contents

List of symbols and abbreviations

EEG	–	Electroencephalogram
BCI	–	Brain-computer interface
ICA	–	Independent component analysis
PDC	–	Partial directed coherence
DTF	–	Directed transfer function
VAR	–	Vector autoregression
MI	–	Motor imaginary

List of Figures

Listings

1 Introduction

Studying of the brain has been an interesting and fascinating subject for many years. The area still has a lot of unanswered questions and attracts lots of scientists all over the world.

A lot of research is dedicated to searching for functional connectivity within the brain on different structural levels - from single neurons to neural assemblies. Functional connectivity is reflected in statistical relationships between brain signals. Signals may be of different nature and may be obtained by different methods such as - electroencephalography (EEG), magnetoencephalography (MEG), functional magnetic resonance imaging (fMRI) etc.

For a long time electroencephalograms (EEG) have been considered to contain quite a little amount of information for the purposes of research of how brain is functioning. (It was thought, metaphorically, that studying brain from EEG is similar to studying the structure of a train from the sounds it makes.) EEG was considered to be some kind of byproduct of the brain, which can't be decoded. But 20 years of brain-computer interface (BCI) research and newly developed mathematical methods have nevertheless showed that EEG bears rather delicate information. There is quite a number of phenomena that an electroencephalogram reflects: intentions (e.g. of movements), emotions, imagination of simple pictures, current tasks, etc.

There were many methods designed to investigate functional connectivity. At first, there was method of directed coherence [29] used for studying relations between two channels of bivariate autoregressive process. Then it was applied to clinical problems and later to research interdependence between two cerebral hemispheres [30]. More recently, Geweke's spectral measures were used to detect causal influences in the feline visual cortex [31].

A whole new approach was recently proposed, that is to use independent component analysis (ICA) methods to study functional brain connectivity. EEG electrodes record brain signals, where each electrode picks up a superposition of the activity from sources located in the nearby area of the cortex. ICA methods offer a way to separate signals from different sources and study sources directly.

A question arises though: is it at all adequate to search for a connection between components that are, by definition of the method they were obtained by, independent? Isn't it some kind of a contradiction?

The goal of this work is to study the area of connectivity in brain signals, study different ways to estimate the functional connectivity and use artificial EEG signals to investigate the problem.

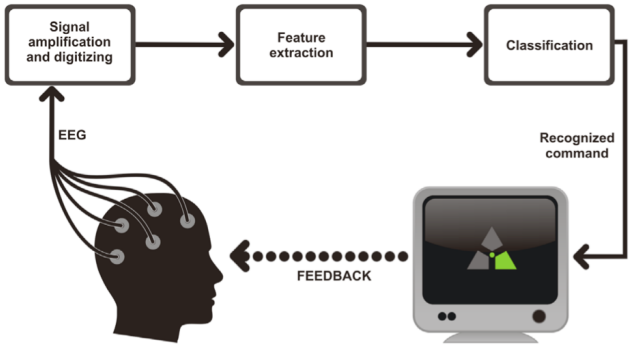

Figure 1: General scheme of an EEG-based BCI [21].

2 Physiological foundation

2.1 Brain-computer interface

A brain-computer interface is an interface used for communication between a brain and a computer without using the peripheral nervous system, i.e. without conscious movement control. "The primary goal of research on BCIs is to enable basic communication for subjects unable to communicate by normal means due to neuro-degenerative diseases such as amyotrophic lateral sclerosis (ALS)" [3]. BCIs can be invasive (such as brain implants, which are used e.g. to treat acquired blindness), partially invasive, non-invasive (based on magnetoencephalography, functional magnetic resonance imaging, electroencephalography). Example of such non-invasive EEG-based BCI is shown on figure 1.

Aside from the fact that signals are obtained using EEG, the picture is quite general. There are many ways, as outlined above, to gather data. For example by measuring of brain hemodynamic activity (BOLD - blood oxygen level dependent signal). Minor disadvantage of this approach is that the characteristic time of detecting changes of hemodynamic activity is several seconds, whereas detecting electrical activity takes only tens of milliseconds. EEG is therefore a very useful tool for BCIs working nearly in real time.

Working in real time is of no advantage in case there are no ways to decipher the signals gathered. Feature extraction is the crucial part in this scheme. There is a wide area of research dedicated to discovering functional brain connectivity. This work is based on one of those ways, specifically one that was proposed by several fellow researches in the field [1], [11] – dividing data obtained via EEG into independent components, which represent single sources of brain electrical activity. Sources are considered to coincide with biologically defined areas of the cortex responsible for certain tasks.

There is also a wide subfield of research dedicated to motor imaginary (MI). That is, first of all, because of its high usefulness. Results that will allow to reliably recognize certain motor imaginary tasks, can be immediately used in brain-computer interfaces: mapping MI tasks to

real-world tasks will allow them to be executed by a machine unit. That has a great application in the area of rehabilitation of patients that aren't capable of movement by themselves.

2.2 Sources of electroencephalography

Electroencephalography (EEG) is an noninvasive electrophysiological method to record electrical activity of the brain. An EEG device consists of several electrodes that are placed along the scalp. EEG measures voltage potentials at various locations on the scalp (in the order of μV) [2]. But the EEG signal is not generated directly under the electrodes. They are generated rather by local field potentials of many distinct cortical domains, where the domain is a patch of the cortex of an unknown area. Pyramidal cells being reliable sources of local potentials are located radially relative to the cortical surface and are near parallel, therefore their local field potentials are summed up to a 'far-field' potential and projected to the scalp electrodes. These far-field potentials are called "current dipoles" and are well established model of neural activity [2]. If pyramidal cells were not near parallel but instead were located chaotically, those local potentials would cancel each other out and prevent the potentials from being detected. From that it follows that EEG data recorded on a single electrode are a superposition (or in another words – a weighted linear mixture) of underlying cortical source signals – current dipoles. [1] Weights of single sources are determined by their distance and position relative to the electrode and the type of the tissue the signal goes through (cortex, cerebral-spinal fluid, skull, and skin). The latter matters due to the different electrical properties of each "material". EEG is considered to have quite low "spatial resolution". This term is used in few different meanings:

- Level of accuracy, with which the position of a single source may be determined;
- Distance between two sources that is necessary for them to be seen as different sources;
- Amount of sources that can be determined from entire data.

Even though it's been this way in the past, new techniques for EEG analysis significantly improve all three aspects of EEG spatial resolution. [1]

2.3 EEG forward problem

Mathematically, the EEG forward problem is "finding, in a reasonable time, the potential $g(\mathbf{r}, \mathbf{r}_{dip}, \mathbf{d})$ at an electrode positioned on the scalp at a point having position vector $\mathbf{r}$ due to a single dipole with dipole moment $\mathbf{d} = d\mathbf{e}_d$ (with magnitude d and orientation $\mathbf{e}_d$), positioned at $\mathbf{r}_{dip}$" [2].

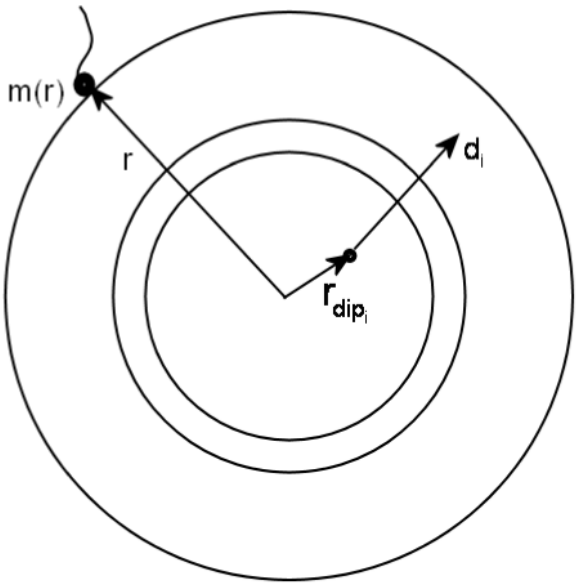

Figure 2: A three layer head model [2].

Data matrix recorded from EEG can be written this way (assuming the dipoles are oriented normal to the surface):

$$M = \begin{pmatrix} \mathbf{g}(\mathbf{r}_1, \mathbf{r}_{dip_1})\mathbf{e}_1 & \cdots & \mathbf{g}(\mathbf{r}_1, \mathbf{r}_{dip_p})\mathbf{e}_p \\ \vdots & \ddots & \vdots \\ \mathbf{g}(\mathbf{r}_N, \mathbf{r}_{dip_1})\mathbf{e}_1 & \cdots & \mathbf{g}(\mathbf{r}_N, \mathbf{r}_{dip_p})\mathbf{e}_p \end{pmatrix} = \mathbf{G}(\{\mathbf{r}_j, \mathbf{r}_{dip_i}, \mathbf{e}_i\})\mathbf{D}, \tag{1}$$

where $\mathbf{G}$ is a gain matrix and $\mathbf{D}$ is a matrix of dipole magnitudes at different time instants [2]. Incorporating noise leads to

$$M = GD + n \tag{2}$$

In practice, this problem is solved by measuring a potential between an electrode and a reference (another electrode or average reference) [2].

2.4 Inverse source localization problem

Finally, a term strongly connected with the area of EEG analysis, is inverse source localization problems. The name speaks for itself: from input EEG data it's necessary to extract cortical distribution of the above-mentioned far-field potentials as accurately as possible. Using the notation mentioned in the previous section, "the inverse problem then consists of finding an estimate $\hat{D}$ of the dipole magnitude matrix given the electrode positions and scalp readings M and using the gain matrix G calculated in the forward problem" [2]. A dipole in the most general

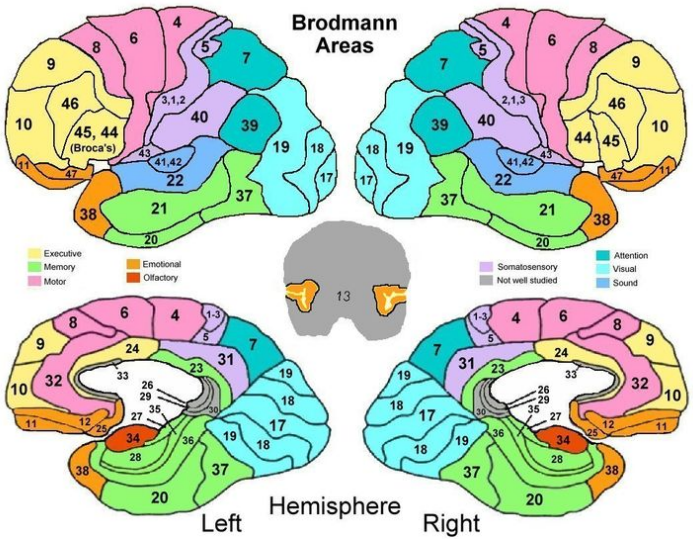

Figure 3: Brodmann areas

way is specified by its location (spatial coordinated (x, y, z)) and dipole moment components (orientation angles (θ, ϕ) and strength d).

As a general problem, it's not at all simple. The main problem, which can arise, is that the data might be underdetermined as number of dipoles is much greater than number of electrodes. Or, for example, far-field potentials from two sources positioned in the different directions on the opposite sides of the cortex will cancel each other out and neither of them will be appear in the EEG data.

Nevertheless there are several facts and assumptions that can greatly simplify the given problem. First of all it's been for a long time now observed that the cortex consists of compact areas that are responsible for certain functions. These areas are called Brodmann areas, and were originally defined and numbered by the German anatomist Korbinian Brodmann. Areas were distinguished based on different cell structure. There are 52 Brodmann areas in total. A simple scheme of Brodmann areas is shown in figure 3.

Another helpful assumption is also related to physiological properties: across a sufficient amount of time, signals from different activity sources have high degree of independency in the time domain. Different mental tasks engage different areas of the cortex, which means that measuring EEG signals from specific source at a given moment allows no conclusion about activities of a different source at the same time, which in turn means that the sources are time-wise independent. Both those assumptions together are enough to distinguish signals from different source areas of the cortex, assuming that their contribution to the scalp data are highly independent over time. Basically, "EEG scalp signals may be modeled as the sum of distinct, phase-independent, and spatially stationary signals from cortical patches (or coupled patch pairs)" [1]. This idea has given a big impulse to the development of a new field in signal processing - independent component analysis, also known as blind separation [1].

2.5 Independent component analysis

Independent component analysis is a general name for a group of methods that allow to separate signals into, as the name suggests, independent components. The methods of this group use only time course information in the process and disregard details of the chosen model, which makes them 'blind' [1]. There are several known implementations of ICA algorithms that are worth mentioning: JADE [4], infomax ICA [5], fastICA [6], SOBI [7]. Scott Makeig and his research group also contributed to the matter by creating an open source Matlab environment called EEGLAB, which provides ICA algorithms ready to use. The environment is freely available online [1].

In [20] and [21] there was proposed alternative approach to inverse source localization problem, which was extensively based on independent components analysis.

Prerequisites for obtaining relatively good results with independent component analysis algorithms are two assumptions and three effects of mixing source signals. Assumptions are the following:

1. The source signals are temporally independent.
2. The values within each channel have non-Gaussian distribution.

Three properties that allow successful 'unmixing':

1. Dependence: even though source signals are independent, their mixtures are not due to them sharing the same source signals.
2. Normality: according to the central limit theorem, the distribution of a sum of independent random variables with finite variance tends towards a Gaussian distribution. If the source signal is being considered a random variable (which EEG signal may very well be), it has the desired property.
3. Complexity: the temporal complexity of any signal mixture is greater than that of its simplest constituent source signal [6].

ICA finds independent components by maximizing statistical independence of the estimated components. Two widely used definitions of independence are:

- Minimization of mutual information.
- Maximization of non-Gaussianity.

The input to the ICA algorithm is simply a matrix $n \times m$, which represents a multichannel EEG signal, where n is the number of channels (i.e. the number of electrodes) and m is the length (measured in number of time points) of a signal. Ordering of channels is irrelevant. ICA performs separation based on the criterion that resulting time series should be maximally

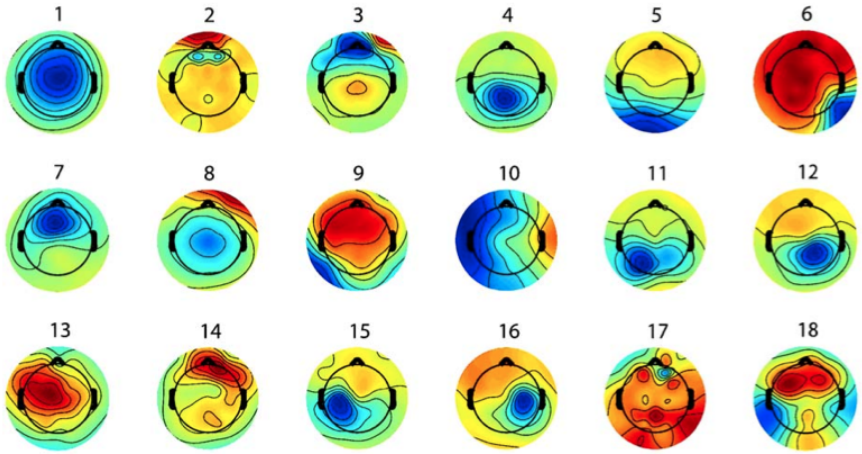

Figure 4: Examples of sources [1].

independent. The output is $n \times n$ matrix W is a "'mixing' matrix whose columns contain the relative weights with which the component projects to each of the scalp channels, i.e., the IC scalp map" [1]. When multiplied by the original time series X, matrix W^{-1} gives a matrix of independent components:

$$\xi = W^{-1}X, \tag{3}$$

where ξ has the same dimension $n \times m$ as the original signal. Following the rules of linear algebra:

$$X = W\xi \tag{4}$$

To get back to the formal definition, each column of the mixing matrix (W) represents "the relative projection weight at each electrode of a single component source" [1]. In other words, it shows how much a single source contributes to the potential measured on the electrode. It is assumed that sources of electrical activity that can be measured on the scalp are current dipoles distributed inside the brain cortex. Source locations are presumed to be stationary. "That is, the brain source locations and projection maps (W^{-1}) are assumed to be spatially fixed, while their 'activations' (ξ) reveal their activity time courses throughout the input data. Thus, the IC activations (ξ), can be regarded as the EEG waveforms of a single sources" [1]. Every current dipole generates specific potential distribution on the head surface. These potentials are continuous, smooth and have one or two distinctive focuses. Examples of such potentials can be seen on figure 4.

After components have been identified, inverse source localization problem is solved for each of them separately. In this case the problem is reduced to searching for such location and orientation of the current dipole that residual dispersion is minimal.

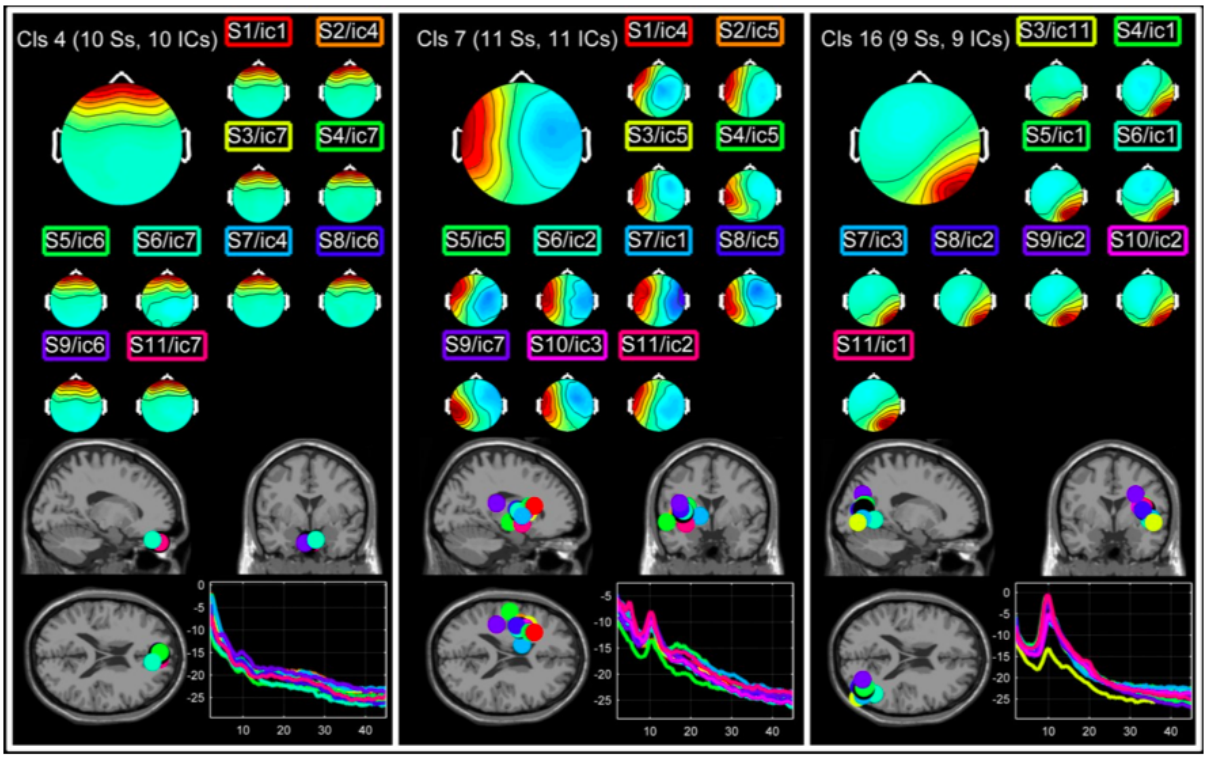

Figure 5: Three clusters computed for one of the subjects. The first cluster (Cls4) corresponds to eye blinks. The second cluster (Cls7) shows ICs with left-parietal alpha range activity. The third cluster (Cls16) shows right occipital alpha activity [19].

ICA methods can be complete (return as much components as is present in the input data) as well as overcomplete (are capable of finding more components than the number of channels in the input data). The latter are rather mathematically complicated and require additional assumptions.

A base hypothesis is that sources of brain electrical activity are stable and also can be observed in different people. That being said, it's nevertheless necessary to take into account head geometry, which will result in possible variations of the sources. During experiments the proof of that concept might be also compromised by changes of electrode placement or specific noise during the experiment. Scott Makeig, for example, showed [19] that sources found using ICA are similar for a single person during different measurements. In his paper, which contributes to the hypothesis being true, he describes an experiment consisting of 11 20-minute measurements performed in the course of 5 weeks. Blind separation was performed on the data and then clustered using customized k-mean function. Figure 5 shows three such clusters.

3 Measures of brain connectivity

Brain connectivity being researched on different levels of central nervous system – from single neurons to whole functional blocks – is one of the key directions of the current neuroscience. In order to properly define connectivity it's necessary to introduce a mathematical model for the signal and some quantity measures and statistics based on this model These measures are called brain connectivity estimators. In the time domain, it's cross-correlation functions among all channels and autocorrelation functions for each channel. In the frequency domain, it's also cross-correlation and autocorrelation, which give basis for computation of the coherence function. This chapter is dedicated to the mathematical apparatus used for quantitative description of brain connectivity.

3.1 Vector autoregressive model

Vector autoregressive model (VAR-model) is a linear mathematical model used to express linear dependencies among multiple time series. The model describes time series in such a way that every ith value (or a tuple in case of multiple channels) is a linear combination of the previous p values of the time series, p being the order of the series. General form of vector autoregressive model looks the following way:

$$Y(t) = A_1 y(t-1) + A_2 Y(t-2) + \cdots + A_p Y(y-p) + N(t) \tag{5}$$

Matrices A_1, A_2, ..., A_p are coefficient matrices, which are constant throughout the time series and $N(t)$ is the noise.

Conditions for VAR-model applicability:

- Normality. A multi-channel signal, which can be modeled using the vector autoregressive model shall have normal distribution, because signal $x(t)$ is linearly bounded with white Gaussian noise $e(t)$ [27]. That is, it's necessary to test that joint probability distribution of all channels of a signal has normal distribution across all dimensions. In practice it's usually done only by verifying normal distribution of single channels [28].
- Stationarity. Another condition is weak stationarity of a signal. For Gaussian vector stochastic process it means that signal average doesn't depend on the value of t. In other words, VAR-model holds for any segment of the length $P + 1$ [17].

VAR-model will be used in this work to model EEG signals.

3.2 AR fitting

In case that input is a signal, it's necessary to fit the signal into a model, i.e. find such matrices A_1, A_2, ..., A_p that equation (5) best fits the signal. One of several existing algorithms for the described fitting, introduced by Möller [9], is listed below.

Starting values are:

$$\hat{\Theta}_0 = 0 \tag{6}$$

$$C_0^{(K)} = I_{M\times p} \tag{7}$$

$$C_n^{(0)} = \frac{1}{1-c} C_{n-1}^{(K)}, \tag{8}$$

where $n = 1, 2, 3, \ldots$ is the iteration step.

$$C_n^{(k)} = C_n^{(k-1)} \left(I_{Mp} - \frac{W_n^T(k,\cdot) W_n(k,\cdot) C_n^{(k-1)}}{W_n(k,\cdot) C_n^{(k-1)} W_n^T(k,\cdot) + 1} \right), \tag{9}$$

where $k = 1, \ldots, K$.

$$K_n = W_n C_n^{(K)} \tag{10}$$

$$Z_n = Y_n - W_n \hat{\Theta}_{n-1}^T \tag{11}$$

$$\hat{\Theta}_n = \hat{\Theta}_{n-1}^T + Z_n^T K_n \tag{12}$$

In the above algorithm $W_n \in \mathbb{R}^{K\times Mp}$, $W_n = (Y_{n-1}, \ldots, Y_{n-p})$, contains the last p observations of the signal ($Y_{n-j} = 0$, for $j \geq n$) and $W_n(k,\cdot)$ denotes the k-th row of W_n. Weighting factor $(1-c)^{n-i}$, where $0 \leq c < 1$ serves to assure that distant values are properly "forgotten" [9]. p is the desired order of the fitted model.

3.3 Generating random signals

3.3.1 Generating primitive signals

As stated above, the signal is going to be generated using a vector autoregressive model. In its general form, the signal will satisfy the expression (5). For simplicity of the following proof, let's assume a 1st-order signal:

$$y(t+1) = Ay(t) \tag{13}$$

At this point let's step aside for a minute and look at differential equations. More precisely – a system of differential equations. For simplicity let's imagine a system of three differential

equations, where the coefficients are elements of matrix A from (13):

$$\begin{aligned} y_1' &= a_{11}y_1 + a_{12}y_2 + a_{13}y_3 \\ y_2' &= a_{21}y_1 + a_{22}y_2 + a_{23}y_3 \\ y_3' &= a_{31}y_1 + a_{32}y_2 + a_{33}y_3 \end{aligned} \tag{14}$$

The idea is to show that the signal can be modeled using solutions of a system of differential equations.

Solution of the given system looks the following way:

$$y = C_1 \cdot \mathrm{e}^{\lambda_1 x} \cdot v_1 + C_2 \cdot \mathrm{e}^{\lambda_2 x} \cdot v_2 + C_3 \cdot \mathrm{e}^{\lambda_3 x} \cdot v_3 \tag{15}$$

where λ_1, λ_2 and λ_3 are the eigenvalues of the matrix $\begin{pmatrix} a_{11} & a_{12} & a_{13} \\ a_{21} & a_{22} & a_{23} \\ a_{31} & a_{32} & a_{33} \end{pmatrix}$, which is a characteristic matrix of the system of differential equations, v_1, v_2 and v_3 are eigenvectors and C_1, C_2 and C_3 are real constants.

Let's now take the definition of the derivative:

$$f'(t_0) = \lim_{t \to t_0} \frac{f(t) - f(t_0)}{t - t_0} = \lim_{\Delta t \to 0} \frac{f(t_0 + \Delta t) - f(t_0)}{\Delta t} \tag{16}$$

and for the purposes of the computation assume Δt to be 1. That would change the definition to the following form:

$$f'(t) = \frac{f(t+1) - f(t)}{t + 1 - t}, \tag{17}$$

so

$$f'(t) = f(t+1) - f(t) \tag{18}$$

Let's now combine the system of the differential equations and the definition of the derivative:

$$y'(t) = Ay(t) - y(t) \tag{19}$$

$$\begin{pmatrix} y_1(t+1) \\ y_2(t+1) \\ y_3(t+1) \end{pmatrix} = \begin{pmatrix} a_{11} - 1 & a_{12} & a_{13} \\ a_{21} & a_{22} - 1 & a_{23} \\ a_{31} & a_{32} & a_{33} - 1 \end{pmatrix} \begin{pmatrix} y_1(t) \\ y_2(t) \\ y_3(t) \end{pmatrix} \tag{20}$$

From the above equation it follows that:

$$y'(t) = (A - I) \cdot y(t) \tag{21}$$

So what can be observed here is that first-order differentials in a way allow to make the "connection" between the current and the previous point of a signal. Similarly, second-order differential equations "connect" the current point with the previous 2 points. Finally, n-order differential equations show the dependency between $n+1$ consecutive points. Since (13) and (21) can be considered equivalent, it can be inferred that the signal over time has a form of (15). Therefore the waveform of a signal is directly dependent on the eigenvalues of the matrix A. Substitution of (15) into (13):

$$ve^{\lambda} = Av \tag{22}$$

or

$$(A - e^{\lambda}) \cdot v = 0 \tag{23}$$

From the above equation and the properties of the exponential function it can be deduced that desired eigenvalues are complex number satisfying the condition $|z| < 1$. That means that matrix A has to be built up from eigenvalues and eigenvectors. Let's take into account that square $n \times n$ matrix A can be decomposed into the product of a matrix of its eigenvalues and a matrix of its eigenvectors:

$$A = DVD^{-1}, \tag{24}$$

where D is a square $n \times n$ matrix, where the ith column is its ith eigenvector and V is a diagonal matrix whose diagonal elements are eigenvalues. Eigenvalues are supposed to be generated in pairs (complex number and its conjugate). Eigenvectors may be random, but have to come in pairs (complex vector and its conjugate) as well, in order to correspond to eigenvalues. On figure 6a, there is a primitive artificial signal of 1st order, one channel, 10000 points, with added white noise, generated according to (13), using the procedure described above. Figure 6b depicts its spectrum.

3.3.2 Generating a peak on given frequency

In (15) eigenvalues are tightly connected with the frequencies that are mixed in the signal. By Euler's formula

$$e^{ix} = \cos x + i \sin x, \tag{25}$$

the frequency enclosed in imaginary part of the exponential term directly contributes to frequency spectrum of the signal. Therefore in order to get the peak it's necessary to create a pair of eigenvalues with the desired frequency and high absolute value to highlight the frequency

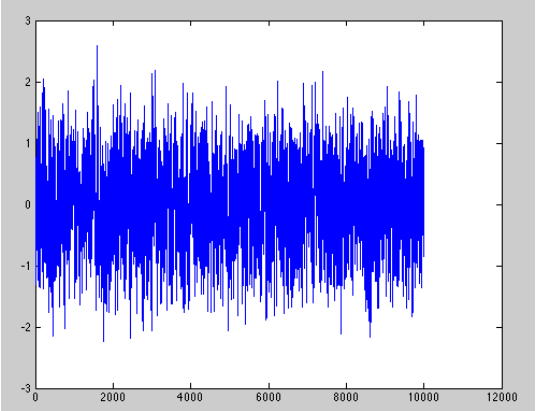

(a) Primitive artificial signal S.

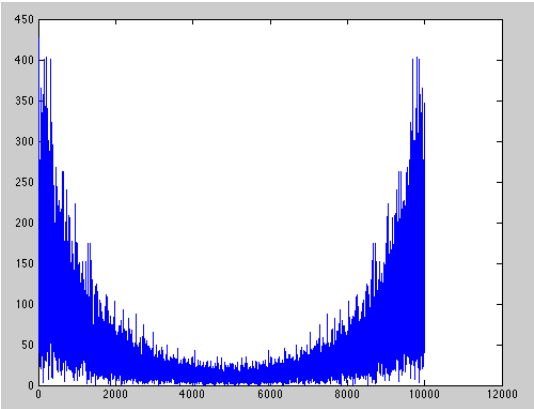

(b) Frequency spectrum of S.

Figure 6: Artificial EEG signal of the 1st order, 10000 points, 1 channel.

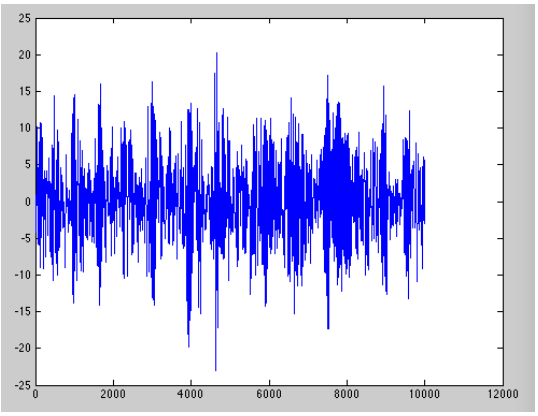

(a) Primitive artificial signal S with a peak.

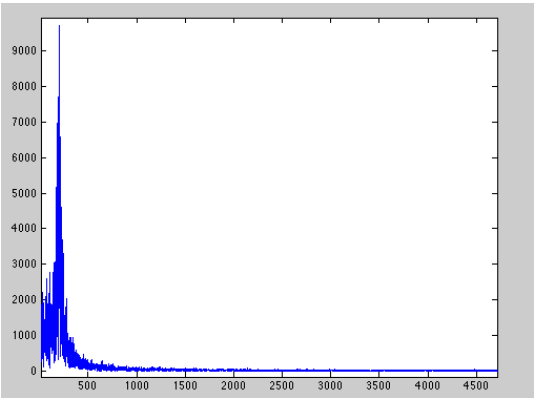

(b) Frequency spectrum of S.

Figure 7: Artificial EEG signal of the 1st order with a peak on 10 Hz, 10000 points, 1 channel.

on the spectrum. Assuming the desired peak to be 10 Hz and sampling frequency 500 Hz, the coefficient of the imaginary part of the eigenvalue should be

$$k = \frac{10 \cdot 2 \cdot \pi}{500}. \tag{26}$$

Since it's necessary for eigenvalues to satisfy $|z| < 1$, it's reasonable to set the absolute value e.g. to 0.999 in order to highlight the frequency on the spectrum. On figure 7a, there is a primitive artificial signal of 1st order, one channel, 10000 points, with added white noise, generated according to (13), using the procedure described above with a peak added on 10 Hz. Figure 7b depicts its spectrum.

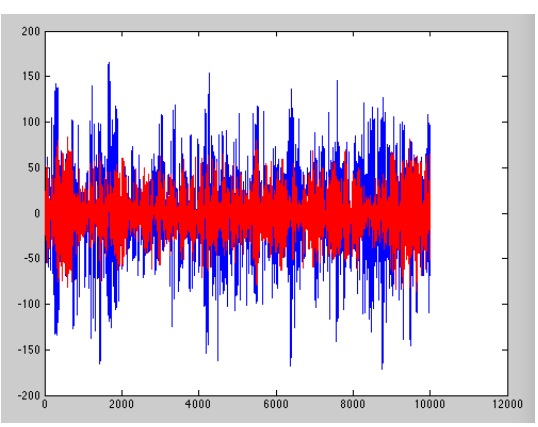

(a) Artificial signal S.

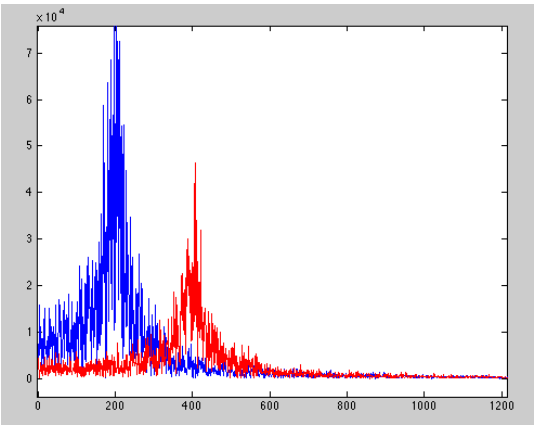

(b) Frequency spectrum of S.

Figure 8: Artificial signal, 2 channels, 10000 points, peaks on 10 Hz and 20 Hz on different channels.

3.3.3 Artificial signals according to Möller and Schack

In the following work there is going to be used slightly different approach, proposed by Möller and Schack [9]. Here is how they propose to do it:

Step 1: Set $A_k^{(0)} = 0$, where $A_k^{(0)} \in \mathbb{R}^{M \times M}$ and $k = 1, \dots p$. Further, set $i = 1$.

Step 2: Generate an arbitrary non-zero matrix $\tilde{\Phi}_i \in \mathbb{R}^{M \times M}$. Compute

$$\Phi_i = ((1 + \varepsilon_i) \mid \lambda_{max}(\tilde{\Phi}_i) \mid)^{-1} \tilde{\Phi}_i \tag{27}$$

where $\lambda_{max}(\tilde{\Phi}_i)$ is the (absolutely) largest eigenvalue of the matrix $\tilde{\Phi}_i$ and $\varepsilon_i > 0$.

Step 3: Compute current parameter matrices from

$$A_1^{(i)} = A_1^{(i-1)} + \Phi_i, \tag{28}$$

$$A_k^{(i)} = A_k^{(i-1)} - A_{k-1}^{(i-1)} \Phi_i, (k = 2, \dots, i) \tag{29}$$

Step 4: If $i < p$, set $i = i + 1$ and return to step 2, else set $A_k = A_k^p$, $(k = 1, \dots, p)$ and stop the iteration.[9]

Epsilon was chosen empirically in order for the signal to resemble an EEG signal. Combined with the previously described approach of generating a signal with a peak on the given frequency, it allows to create a signal depicted on figure 8a, showing an example of such artificial signal with 10 Hz (resp. 20 Hz) peak on 1st (resp. 2nd) channel. Figure 8b shows its frequency spectrum.

This signal from now on will be the main subject of the following research.

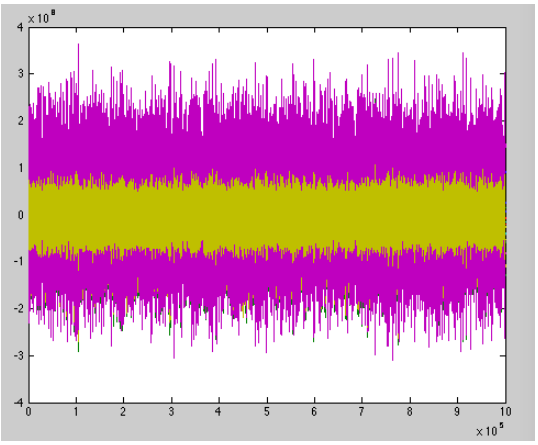

(a) Artificial signal S.

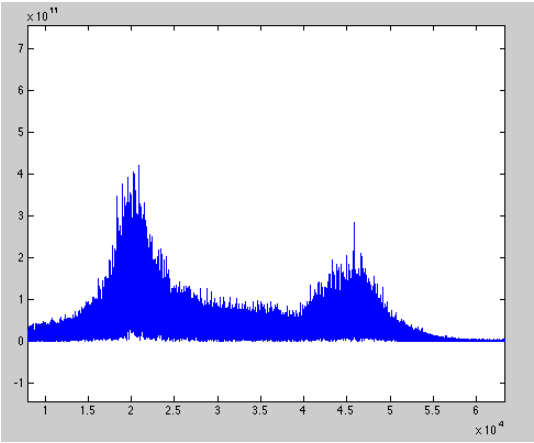

(b) Frequency spectrum of S.

Figure 9: Artificial signal of 25th order, 20 channels, 1000000 points, peaks on 10 Hz and 20 Hz on different channels.

In order to test the stability of the model, a long and higher order signal was generated. It's shown on figure 9a, and next to it, on figure 9b is its frequency spectrum. It can be seen that the signal doesn't diverge, therefore the model is stable.

It was also necessary to verify that the created signal can successfully model EEG sources. In order to do that, the following was done:

1. Three different signals of 2nd order of length 10000 with 2 channels were created.
2. The signals were placed next to each other, thus creating a single 2 channel signal with three different states.
3. As the next step, channels were artificially 'mixed': the signal was multiplied by a random matrix $n \times n$, where n is the number of channels (in this case 2), thus creating a linear mixture, which resembles real EEG signals more closely.
4. ICA was applied in order to see whether initial components are separated.

Components were separated successfully.

3.4 Methods of signal interaction analysis

Let's assume a data set of scalp data of M-channel EEG, N time points long. Each discrete time point n has corresponding m values of electrical potential. Electrical potential is a column-wise vector $x(t) = [x_1(t), x_2(t), \ldots, x_M(t)]^T$, where $x_m(t)$ is the value of electric potential on channel m ($m = 1, 2, \ldots, M$). As has been established above, VAR-model of the p-th order claims that in any time point, t values of electric potentials are represented by the linear combination of the previous p values and of the white gaussian noise vector $e(t) = [e_1(t), e_2(t), \ldots, e_M(t)]^T$ with the

covariance matrix Σ. Most of the brain connectivity estimators are computed in the frequency domain, so it's necessary to show how the signal will look like in the frequency domain. Any times series can be decomposed into series of sine functions of different frequencies and amplitudes, that sum up to the given signal. The mathematical operation for such a decomposition is the Fourier transformation:

$$\int_{-\infty}^{\infty} x(t) \cdot e^{-i\omega t} \mathrm{d}t = x(\omega) \tag{30}$$

The inverse Fourier transformation allows to get a signal from its frequency spectrum:

$$\int_{-\infty}^{\infty} x(\omega) \cdot e^{i\omega t} \mathrm{d}t = x(t) \tag{31}$$

Let's now assume a signal $X' = A \cdot X(t)$, where A is a matrix independent of t. The Fourier transformation of X' is $A \cdot X(\omega)$.

The signal generated in the previous paragraph looks like this:

$$X(t) = A_1 X(t-1) + \cdots + A_n X(t-n) + N(t) \tag{32}$$

In the frequency domain, the signal looks the following way:

$$X(\omega) = A_1 \mathrm{e}^{-i\omega} X(\omega) + \cdots + A_n \mathrm{e}^{-ni\omega} X(\omega) + N(\omega) \tag{33}$$

The above expression can be modified in the following way:

$$(I - A_1 \mathrm{e}^{-i\omega} - \ldots - A_n \mathrm{e}^{-ni\omega}) \cdot X(\omega) = N(\omega) \tag{34}$$

The expression in parenthesis shall be denoted $A(\mathrm{e}^{i\omega})$ or $A(z)$, where z is a function of frequency. Therefore the whole expression takes the form

$$A(\omega) \cdot X(\omega) = N(\omega) \tag{35}$$

Equation (35) is a VAR-model equation (5) rewritten into the frequency domain.

3.4.1 Direct coupling function

Before describing a whole series of estimators in the frequency domain, let's take a look at direct coupling as a measure computed in the time domain. The starting point is the very definition of the VAR model (5). A_i in this equation is a square matrix $m \times m$, where m is the number of channels. Each element $a_{km}(p)$ of these matrices shows how the signal $x_m(t-p)$ from channel m contributes to the signal $x_k(t)$ on channel k. The influence of the m-th channel on channel k is given by the series of coefficients $a_{km}(p)$ for every possible time delay $p = 1, 2, 3, \ldots, P$. The influence is zero if every coefficient $a_{km}(p)$ for $p = 1, 2, \ldots, P$ is zero [17]. Coefficients $a_{km}(p)$ are the basis for computation of directed coupling function (also called direct causal influence).

Directed causal influence of channel m on channel k (denoted $\mathrm{DC}_{k\leftarrow m}$, where the arrow marks the direction of the influence) is computed:

$$\mathrm{DC}_{k\leftarrow m} = \sum_{p=1}^{p=P} a_{km}^2(p) \tag{36}$$

In general, $\mathrm{DC}_{k\leftarrow m} \neq \mathrm{DC}_{m\leftarrow k}$.

3.4.2 Partial directed coherence

First of the brain connectivity estimators described below will be partial directed coherence. In the VAR model rewritten into the frequency domain (35) $X(\omega) = [X_1(\omega), X_2(\omega), \ldots, X_M(\omega)]^T$ is a vector (column vector in a way) of Fourier transformations of the source signal, and $N(\omega) = [N_1(\omega), N_2(\omega), \ldots, N_M(\omega)]^T$ is a column vector of Fourier transformations of white noise. Elements of the complex matrix $A(\omega)$, as can be understood from above, are computed from Fourier transformations of the input matrices A_1, A_2, ..., A_P. Element $A_{km}(\omega)$ of matrix $A(\omega)$ shows, what frequency filter will the mth channel of the signal $X(\omega)$ undergo before it becomes a part of the signal on channel k [17]. Therefore the function $\left|A_{km(\omega)}\right|$ can be used as a measure of directed impact of one channel on another. That fact is used in the definition of a measure called "partial directed coherence" (PDC):

$$\pi_{k\leftarrow m}(\omega) = \frac{|A_{km}(\omega)|}{\sqrt{\sum_{j=1}^{j=M} |A_{jm}(\omega)|^2}} \tag{37}$$

Partial directed coherence was defined by Baccala and Sameshima [22].

For every frequency ω the value of $\pi_{k\leftarrow m}(\omega)$ (which comes from the interval $< 0; 1 >$) indicates impact of channel m onto channel k relative to the impact of the given channels onto all the channels including m and k.

On figure 10, there is a function of partially directed coherence for a previously generated signal for frequencies between 1 and 50 Hz: blue line is PDC function for $k = 1$ and $m = 1$, red line is PDC function for $k = 2$ and $m = 2$, black line is PDC function for $k = 1$ and $m = 2$.

3.4.3 Directed transfer function

Let's denote matrix $A(\omega)^{-1}$ as $H(\omega)$. $H(\omega)$ is called the directed function of a multichannel system [17]. Using that function the equation can be written down as

$$X(\omega) = H(\omega)\dot{N}(\omega) \tag{38}$$

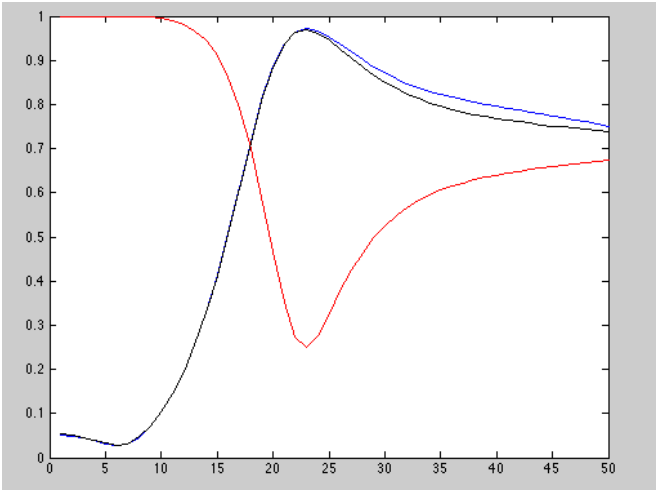

Figure 10: Partial directed coherence.

Each single element of matrix $H_{km}(\omega)$ represents the frequency filters transforming white noise of channel m into legit part of channel k. Elements of matrix H is the basis for directed transfer function (DTF):

$$\theta_{k\leftarrow m}(\omega) = \left|H_{km}(\omega)\right| \tag{39}$$

The spectral density of white noise is independent of the frequency, therefore $\theta_{k\leftarrow m}(\omega)$ basically describes a part of the spectrum of the kth channel, which is influenced by the mth channel directly as well as indirectly (through other channels). Usually, a normalized form is used:

$$\gamma_{k\leftarrow m}(\omega) = \frac{\left|H_{km}(\omega)\right|}{\sqrt{\sum_{j=1}^{j=M}\left|A_{jm}(\omega)\right|^2}} \tag{40}$$

The normalized function shows, how significant is the impact of channel m on channel k compared to the impact of all channels (including m) on channel k.

Directed transfer function in the form outlined above was introduced by Kaminski and Blinowska [23]. DTF shows not only direct, but also cascade flows, for example in case of causal influence of channels in a form $1 \rightarrow 2 \rightarrow 3$, DTF is capable of detecting the connection $1 \rightarrow 3$. In order to distinguish direct from indirect flows, direct Directed Transfer Function (dDTF) was introduced [24]. dDTF is defined as a multiplication of a modified DTF by partial coherence.

3.4.4 Coherence

Another, quite important, measure in the signal processing is spectral coherence. The knowledge of directed function $H(\omega)$ allows to compute the spectral density function $S(\omega)$. $S(\omega)$ is a matrix with the following properties: main diagonal contains signals autospectrums and off-

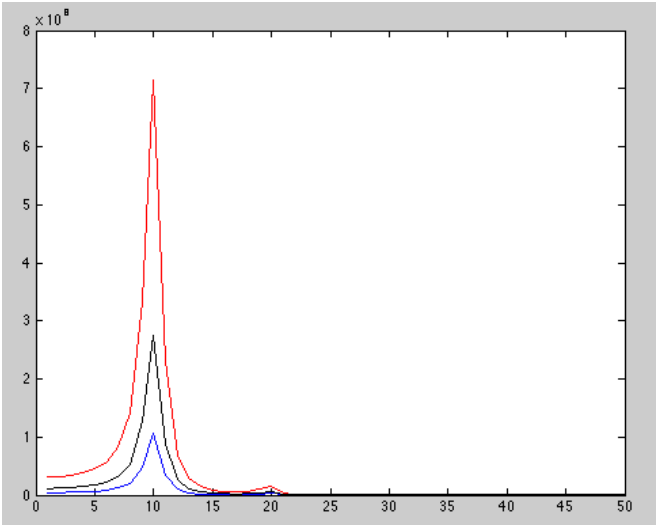

Figure 11: Autospectrum and cross-spectra of artificial signal.

diagonal element represent cross-spectrums. Matrix $S(\omega)$ is the basis for computation of complex coherence function:

$$C_{km}(\omega) = \frac{S_{km}(\omega)}{\sqrt{S_{kk}(\omega)S_{mm}(\omega)}} \tag{41}$$

Whereas regular coherence function is the complex coherence function squared:

$$K^2_{km}(\omega) = \left|C_{km}(\omega)\right|^2 \tag{42}$$

The values of coherence will always satisfy $0 \leq C_{km}(\omega) \leq 1$. Under certain conditions (signals are ergodic and transfer function is linear), coherence can be used to estimate causality.

Autospectrum and cross-spectra for the signal in question are depicted in figure 11.

3.4.5 Granger causality

Granger causality is a measure that not only gives an estimate for a numerical value of causality (like coherence) but also allows to determine the direction of the causal effect. Simple (no math) explanation of Granger causality goes like this: if the knowledge of the past values of the signal x helps to predict future values of the signal y better than knowledge of the signal y alone then x is said to cause y. There is more that one mathematical definition for Granger causality in literature. Schack et al. in [10] present the following description: let's assume multivariate signal X with two channels $X_1 = \{X_1(n)\}$ and $X_2 = \{X_2(n)\}$. In order to show that past values of one signal actually improve prediction of the future values of the second signal, both

signals are fitted with univariate and bivariate autoregression models. For one variable fitting both channels may be described as

$$X_1(t) = \sum_{k=1}^{p} A_1(k) X_1(t-k) + u_1(t), \tag{43}$$

$$X_2(t) = \sum_{k=1}^{p} A_2(k) X_2(t-k) + v_1(t), \tag{44}$$

where the prediction errors u_1 and v_1 depend only on the past of the signal itself. For bivariate modeling

$$X_1(t) = \sum_{k=1}^{p} B_{11}(k) X_1(t-k) + \sum_{k=1}^{p} B_{12}(k) X_2(t-k) + u_2(t) \tag{45}$$

$$X_2(t) = \sum_{k=1}^{p} B_{21}(k) X_1(t-k) + \sum_{k=1}^{p} B_{22}(k) X_2(t-k) + v_2(t) \tag{46}$$

the prediction is based on the past of the signal itself and additionally on the past of the second signal. Quantitative measure of the accuracy of prediction may be expressed as the variance of the prediction errors. For univariate it's

$$\Sigma_{X_1|X_1^-} = \mathrm{var}(u_1) \tag{47}$$

and

$$\Sigma_{X_2|X_2^-} = \mathrm{var}(v_1) \tag{48}$$

For the bivariate modeling it's

$$\Sigma_{X_1|X_1^-,X_2^-} = \mathrm{var}(u_2) \tag{49}$$

and

$$\Sigma_{X_2|X_2^-,X_1^-} = \mathrm{var}(v_2) \tag{50}$$

If the signal $X_2(t)$ causes signal $X_1(t)$, the variance of the prediction error should decrease for bivariate model, where past values of the signal $X_2(t)$ are taken into account for the prediction of the future values of $X_1(t)$. Granger causality of X_2 to X_1 is then expressed as a measure of linear feedback [26]:

$$F_{X_2 \to X_1} = \ln \frac{\Sigma_{X_1|X_1^-}}{\Sigma_{X_1|X_1^-,X_2^-}} \tag{51}$$

Respectively, the Granger causality of X_1 to X_2 is

$$F_{X_1 \to X_2} = \ln \frac{\Sigma_{X_2|X_2^-}}{\Sigma_{X_2|X_1^-,X_2^-}} \tag{52}$$

The maximum of both terms

$$F_{X_1 X_2} = \max\{F_{X_2 \to X_1}, F_{X_1 \to X_2}\} \tag{53}$$

represents a simple measure for the strength of directional and/or bi-directional interaction [10].

Another way of computing was presented by Kaminski et al. [12]. Fourier transform was used on (45) and (46) to examine causal relations in the spectral domain. It leads to

$$\begin{pmatrix} A_{11}(\omega) & A_{12}(\omega) \\ A_{21}(\omega) & A_{22}(\omega) \end{pmatrix} \begin{pmatrix} X_1(\omega) \\ X_2(\omega) \end{pmatrix} = \begin{pmatrix} u_2(\omega) \\ v_2(\omega) \end{pmatrix} \tag{54}$$

By rewriting this equation into

$$\begin{pmatrix} X_1(\omega) \\ X_2(\omega) \end{pmatrix} = \begin{pmatrix} H_{11}(\omega) & H_{12}(\omega) \\ H_{21}(\omega) & H_{22}(\omega) \end{pmatrix} \begin{pmatrix} u_2(\omega) \\ v_2(\omega) \end{pmatrix} \tag{55}$$

the transfer matrix is obtained:

$$\begin{pmatrix} H_{11}(\omega) & H_{12}(\omega) \\ H_{21}(\omega) & H_{22}(\omega) \end{pmatrix} = \begin{pmatrix} A_{11}(\omega) & A_{12}(\omega) \\ A_{21}(\omega) & A_{22}(\omega) \end{pmatrix}^{-1} \tag{56}$$

The computation is similar to one given in the previous subsection. Granger causality from channel j to channel i is then defined in terms of the diagonal elements of the transfer matrix [25]:

$$I^2_{j \to i} = |H_{ij}(\omega)|^2 = \frac{|A_{ij}(\omega)|^2}{|A(\omega)|^2} \tag{57}$$

4 Results

4.1 Straight-forward decorellation

From the definition of the VAR model it follows that any signal generated according to that model has interconnected channels, which means that the signal is correlated. Covariance of that signal is:

$$C =< X \cdot X^T > \tag{58}$$

The idea now is to rotate the base of a signal, so it becomes uncorrelated:

$$X' = V \cdot X \tag{59}$$

The uncorrelated signal has to fulfill the following condition:

$$X'(X')^T = I, \tag{60}$$

which leads to

$$VXX^TV^T = I, \tag{61}$$

where $XX^T = C$. By the rules of linear math:

$$C = V^{-1} \cdot V^{-T} \tag{62}$$

Denoting matrix V^{-1} as LW we obtain

$$C = (LW)(LW)^T \tag{63}$$

which is the definition of Cholesky decomposition. Therefore rotating matrix V can be computed from Cholesky decomposition of covariance matrix of the initial signal.

All the measures of the uncorrelated signal X' such as partial directed coherence, can be easily obtained from the measures of the original signal by proper multiplying by V:

$$A'(z) = VA(z)V^{-1} \tag{64}$$

$$H'(z) = VA(z)^{-1}V^{-1} \tag{65}$$

$$S'(z) = VS(z)V^T \tag{66}$$

Now, in order to compare measures of connectivity for original and de-correlated signal, the following was done:

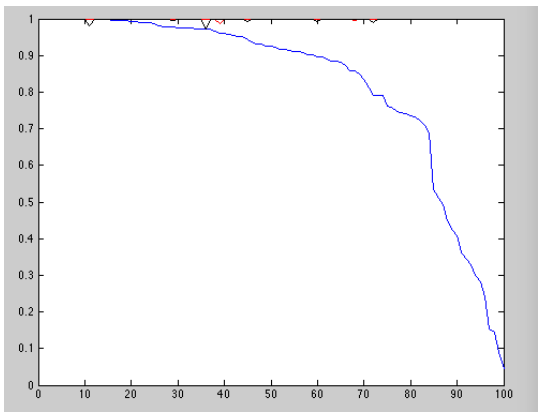

(a) Original signal.

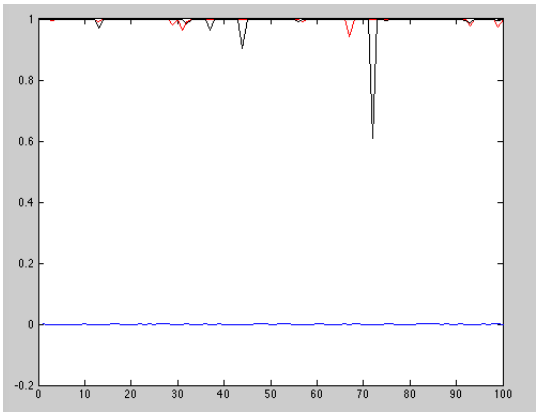

(b) Rotated signal.

Figure 12: Connectivity measures for original and rotated signal. Blue line depicts correlation, red line shows covariance for 10 Hz, black line show covariance for 20 Hz.

1. 100 different signals were generated with the following properties: 10000 points, 2 channels, peaks 10 Hz and 20 Hz on different channel;

2. For each signal the following measures were written down: correlation between 1st and 2nd channel, coherence between 1st and 2nd channel for 10 Hz, coherence between 1st and 2nd channel for 20 Hz;

3. Each signal was rotated according to the procedure described above;

4. Same measures were recorded as it's been done for the original signal.

Comparison of the measures is demonstrated in figures 12a and 12b.

The computation proves that channels with zero coherence can have non-zero connectivity measures.

4.2 Coherence of the filtered signal

Filtering is a procedure that removes some unwanted components from a signal. It's necessary to consider filtering methods because it is often needed to filter an EEG signal (e.g. from noise) before it will be processed by feature extraction procedures. Thus, it's necessary to make sure that the connectivity estimators remain the same.

Filtering is considered in the frequency domain (though it's not restricted to the frequency domain in general case). Since most of the connectivity estimators come from matrices A_1, A_2, $\ldots$, A_p, which are different after filtering is performed, it's necessary to take appropriate steps to compute them. Steps to compute brain connectivity estimators on filtered signal are these:

1. Computing the frequency spectrum using Fast Fourier Transformation.

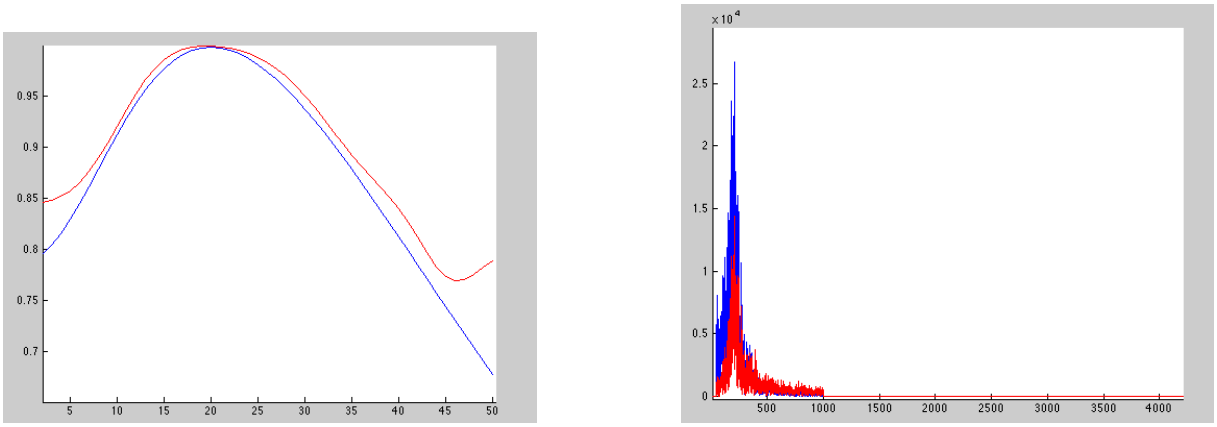

(a) Coherence.

(b) Frequency spectrum of filtered signal.

Figure 13: On the left - comparison of original (blue line) and filtered (red line) coherence. All frequencies before 2 and after 50 Hz were filtered. On the right - frequency spectrum of both channels of the filtered signal.

2. Setting unwanted frequencies to zero.
3. Performing inverse Fourier Transformation.
4. Fitting the resulting signal into autoregressive model.
5. Computing coherence from resulting autoregressive model matrices.

Nonetheless, observations suggest that filtration has drastic influence on correct identification of components. So, the hypothesis in this part is that filtration will obstruct proper component identification and non-changed measures. So, the first step was to observe coherence behavior after filtering different bandwidths. Figures 13, 14, and 16 demonstrate the comparison of the original coherence and coherence after filtration. Gray vertical lines mark borders of the untouched bandwidth.

It can be clearly seen, that even though filtration has left a certain band untouched, coherence within the band has changed. Therefore if the connectivity was to be evaluated on the filtered signal, it may lead to incorrect results.

In order to make quantitative conclusion, for each of filtered bandwidths (2-50 Hz, 3-40 Hz, 5-30 Hz) the following process was conducted:

1. 100 signals were generated, 2 channels, 10th order, 2 peaks 10 and 20 Hz on different channels.
2. Each signal was filtered, leaving certain bandwidth untouched.
3. Coherence was computed for the filtered and non-filtered signals.

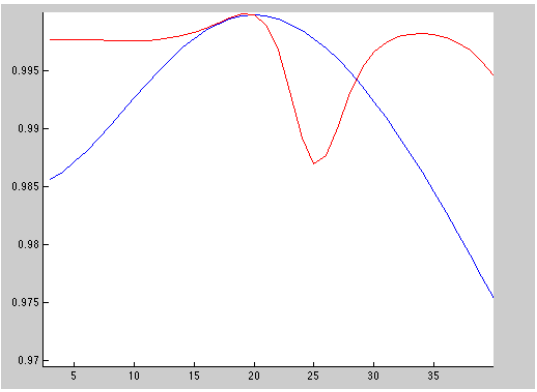

(a) Coherence.

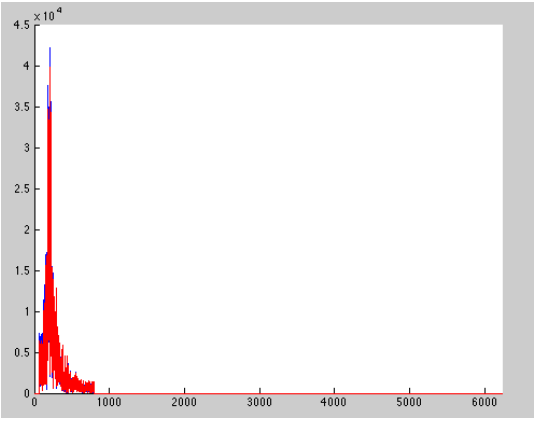

(b) Frequency spectrum of filtered signal.

Figure 14: On the left - comparison of original (blue line) and filtered (red line) coherence. All frequencies before 3 and after 40 Hz were filtered. On the right - frequency spectrum of both channels of the filtered signal.

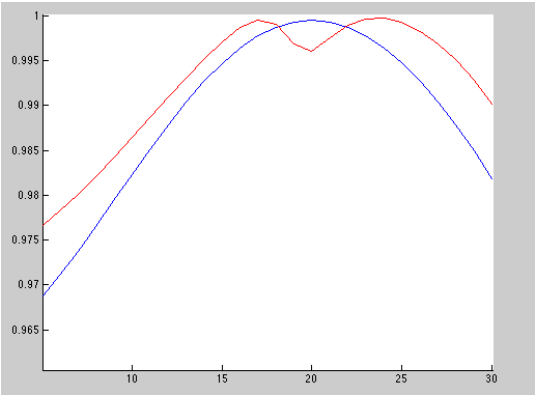

(a) Coherence.

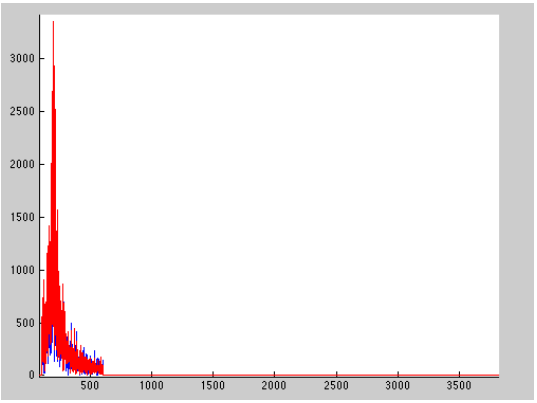

(b) Frequency spectrum of filtered signal.

Figure 15: On the left - comparison of original (blue line) and filtered (red line) coherence. All frequencies before 5 and after 30 Hz were filtered. On the right - frequency spectrum of both channels of the filtered signal.

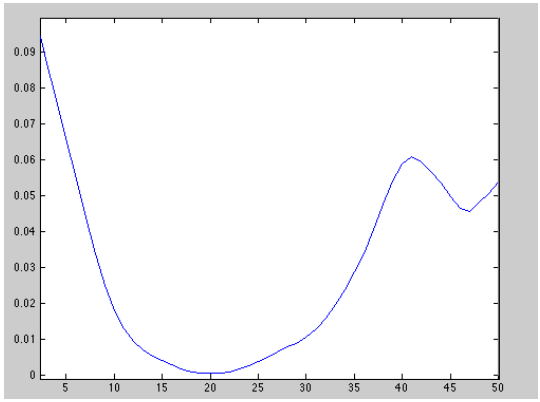

(a) 2-50 Hz

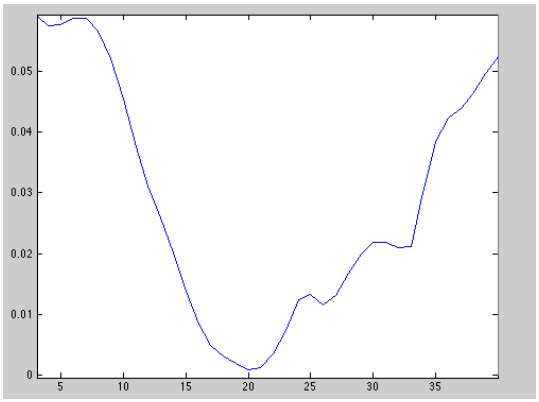

(b) 3-40 Hz

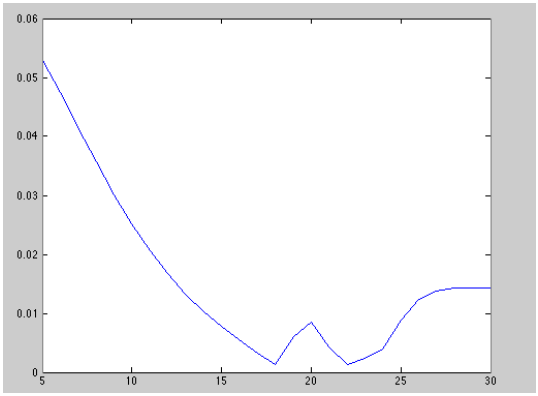

(c) 5-30 Hz

Figure 16: Average difference between coherences of original and filtered signal.

4. For every frequency, an average of absolute difference between the original coherence and the coherence of a filtered signal was computed.

4.3 EEG signal

It was interesting to try to find functional connectivity in real signals. Real signals were chosen from experimental data involving motor imaginary tasks. The signal was digitized with the sampling frequency of 500 Hz. The signal has 276000 time points, where each point corresponds to certain task (period of performing a task is also called "state"). Changing tasks was performed every 10000 time points. Analysis was done in the following way:

1. Independent component analysis algorithm (more precisely - FastICA [6]) was used on the EEG data.

2. Thirteen components were chosen (by the thesis advisor).

3. Part of the signal corresponding to single state was extracted out of the whole signal. Total length of a signal corresponding to the state 1 made 60000 time points.

4. Channels were paired each-to-each.

5. Each pair was then considered to be a bivariate model, for which matrices $A_1, A_2, \ldots, A_p$ were computed. Order $p = 70$ was chosen.

6. For every frequency $\omega \in < 5; 30 >$ coherence was computed.

7. Pairs with significantly high (> 0.3) coherence were given a closer look.

The above process was repeated for all three states contained in the signal.

4.3.1 State 1

The highest coherence for state 1 was found between components 3 and 11. All computed measures are shown in figure 17. Peak in approximately 13 Hz located in the frequency band 10 - 16 Hz, which corresponds to μ-rythm – motor imaginary task.

Components identified by independent component analysis algorithm correspond to sources of electrical activity in the brain. Topoplots (schematic depiction of current dipoles) for components 3 and 11 are shown in figure 18.

4.3.2 State 2

Analysis of state 2 also showed relatively high coherence for components 3 and 11. Also, there was also notably high coherence between components 2 and 6. Peak on approximately 11 Hz can not be exactly identified as μ-rythm (motor imaginary – 10-16 Hz) or α-rythm (eye movements – 8-12 Hz) as the bands overlap. Connectivity estimators are shown in figure 19. Topoplots for these components are shown in figure 20.

4.3.3 State 3

Analysis of the portion of a signal corresponding to state 3 didn't reveal any significant connections. Although, there were few pairs found that demonstrated values of coherence a little over 0.1. Coherence, auto- and cross-spectra and partial directed coherence are depicted in figures 21 (components 2 and 5) and 22 (components 4 and 8).

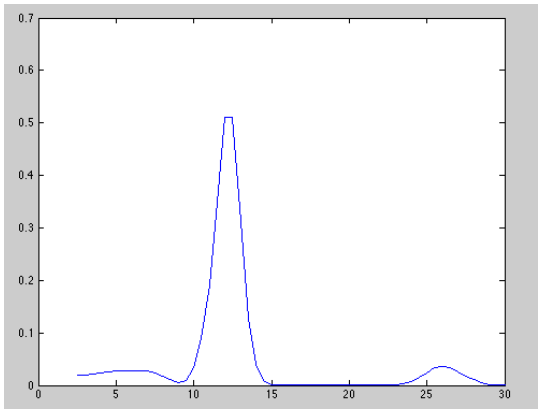

(a) Coherence.

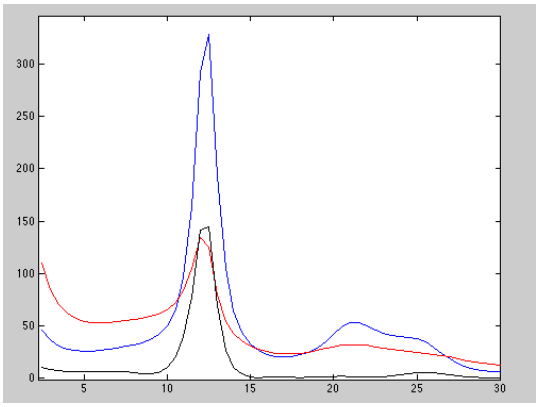

(b) Auto- and cross-spectra. Blue (resp. red) shows auto-specturm of the component 3 (resp. 11). Black line shows cross-spectrum.

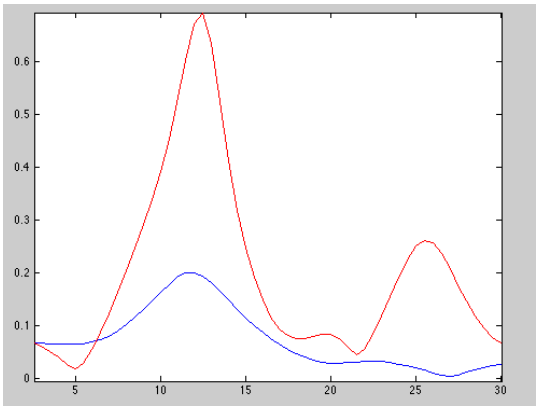

(c) Partial directed coherence. Blue line depicts influence of component 3 on component 11. Red line vice versa.

Figure 17: Brain connectivity estimators for state 1, components 3 and 11.

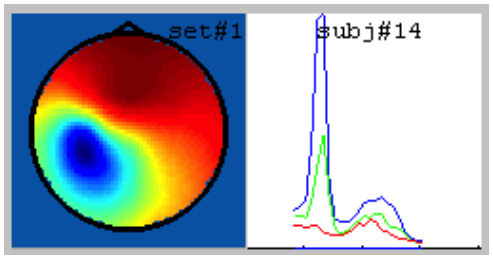

(a) Component 3.

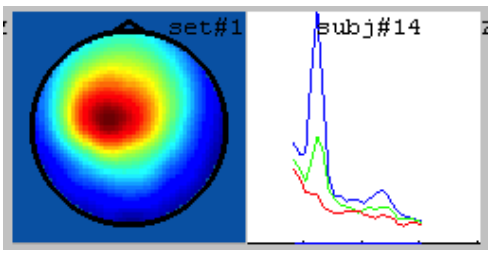

(b) Component 11.

Figure 18: Topoplots for functionally connected components.

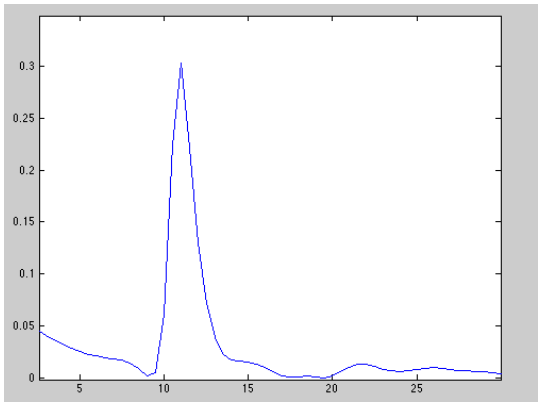

(a) Coherence.

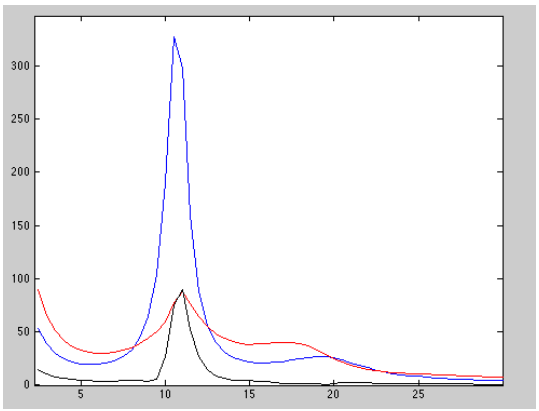

(b) Auto- and cross-spectra. Blue (resp. red) shows auto-specturm of the component 2 (resp. 6). Black line shows cross-spectrum.

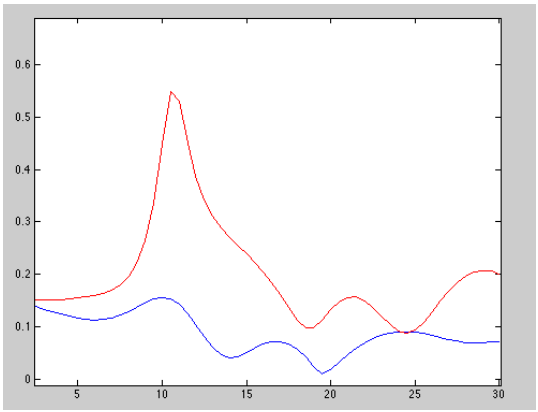

(c) Partial directed coherence. Blue line depicts influence of component 2 on component 6. Red line vice versa.

Figure 19: Brain connectivity estimators for state 2, components 2 and 6.

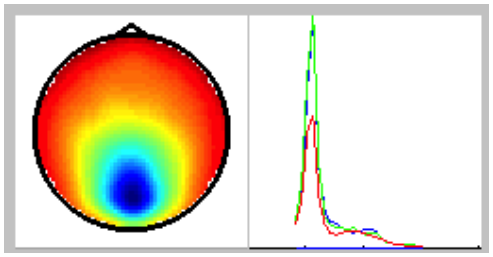

(a) Component 2.

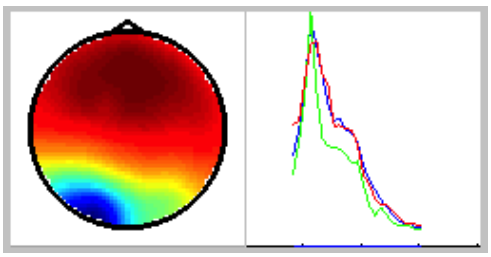

(b) Component 6.

Figure 20: Topoplots for functionally connected components.

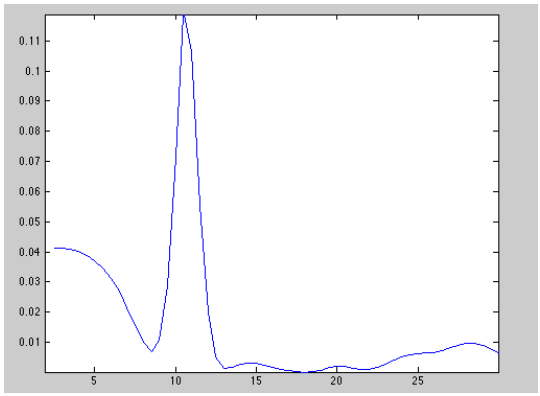

(a) Coherence.

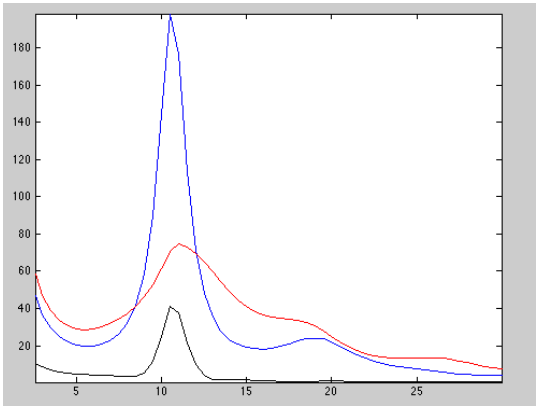

(b) Auto- and cross-spectra. Blue (resp. red) shows auto-specturm of the component 2 (resp. 5). Black line shows cross-spectrum.

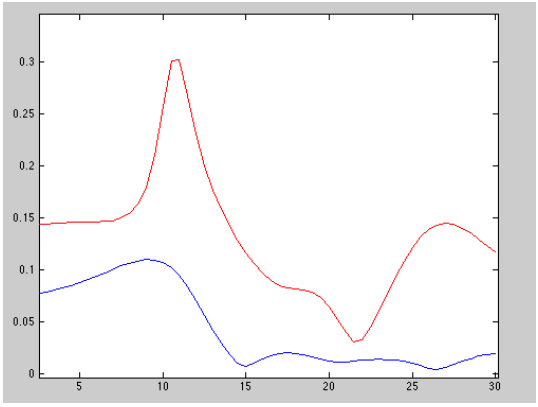

(c) Partial directed coherence. Blue line depicts influence of component 2 on component 5. Red line vice versa.

Figure 21: Brain connectivity estimators for state 3, components 2 and 5.

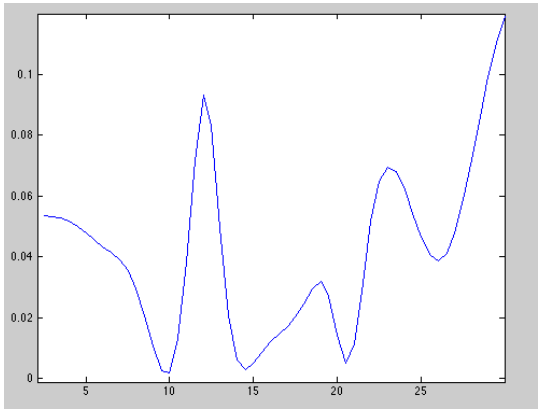

(a) Coherence.

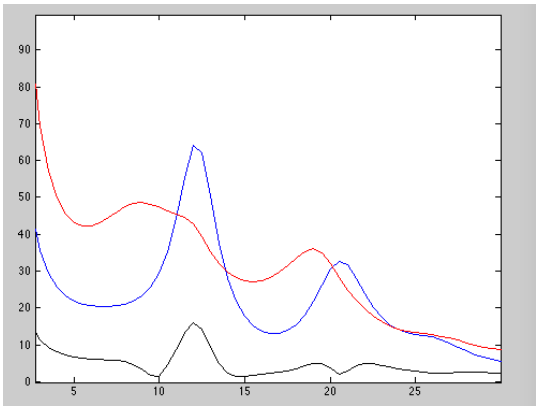

(b) Auto- and cross-spectra. Blue (resp. red) shows auto-specturm of the component 4 (resp. 8). Black line shows cross-spectrum.

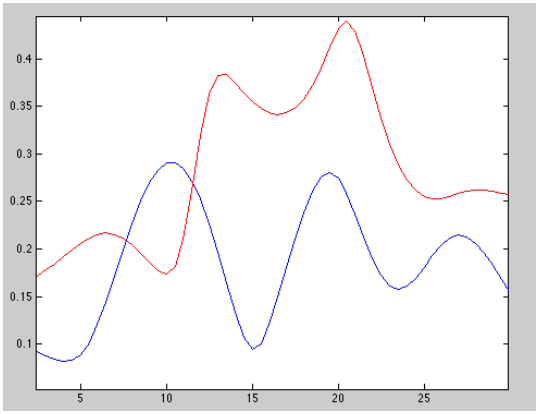

(c) Partial directed coherence. Blue line depicts influence of component 4 on component 8. Red line vice versa.

Figure 22: Brain connectivity estimators for state 3, components 4 and 8.

5 Realization and implementation details

Most of the computations listed in the chapter 3 were actually realized. MATLAB R2014a was used due to its extensive mathematical library. Code consists mainly of single functions that are later used in more complicated functions. MATLAB is capable of storing all used variables in its workspace until they are overwritten, so no special code structure was required. All-in-all submitted code isn't considered to be a working program available for distribution. It's more of a series of work scripts supporting mathematical computation throughout this work.

5.1 Generating random signal

First step was to generate matrix A, which was responsible for a peak on certain frequency.

```
function A = generateA(size, peak)
   p = randperm(size);
   Sfrq = 500; %sampling frequency
   d = zeros([1 size]);
   D = zeros([size size]);

   %create one pair of complex numbers close to 1
   w = 0.99;
   k  = peak*2*pi/Sfrq;
   d(p(1)) = w*exp(complex(0, k));
   d(p(2)) = w*exp(complex(0, -k));
   eigv = complex(rand(size,1),rand(size,1));
   D(:, p(1)) = eigv;
   D(:, p(2)) = conj(eigv);

   %create the rest close to 0
   for i = 1:2:size
      w = rand;
      .
      .
      .
   end
```

Listing 1: Creating of the matrix A

Listed part of the code shows generation of the vector d, which is going to represent a diagonal in the matrix of the eigenvalues. At first the pair of randomly placed complex numbers responsible for the peak is generated. After that the rest is generated randomly taking into

account parity of value, which represents the size (aka number of channels). In case it's odd, the last eigenvalue is made to be non-complex.

Next part is careful implementation of Möller&Schack algorithm according to [9]. Input is a $n \times n \cdot p$ matrix, where n is a number of channels and p is a model order. Function is obviously flexible enough to handle input for any number of channels and any order.

```
As = zeros ([nChannels, order*nChannels]);
for i = 1:order
    Asprev= As;
    FIwave = Fiwave(:, (i-1)*nChannels+1:i*nChannels);
    [u, d] = eig(FIwave);
    w = max(abs(diag(d)));
    Fi = FIwave / ((1 + eps(i)) * w);
    As(:, 1:nChannels) = Asprev(:, 1:nChannels) + Fi;
    for j = 2:i
        As(:, ((j-1)*nChannels + 1):j*nChannels) = ...
            Asprev(:, ((j-1)*nChannels + 1):j*nChannels)...
            - Asprev(:, ((j-2)*nChannels + 1):(j-1)*nChannels)*Fi;
    end;
end;
```

Listing 2: Generating an array of A_i according to Möller and Schack

Matrices A_i are in the above code denoted as Φ_i in order to keep the code consistent with the paper description of an algorithm. Output of this function is a single matrix of a size $n \times n \cdot p$, where n is the number of channels in the desired signal and p is the order on the model. In early stages the code worked correctly, but in later stages and more complex computations it turned out that it doesn't quite fulfill the necessary conditions for desired random signal. VAR generation algorithm for the following computations was provided by the thesis advisor.

Generated A_i matrices are now used to generate signal according to the VAR model (5). In order to simplify generation of one point of a signal down to a single step, VAR model is rewritten into the following form:

$$y(t+1) = Ay(t) + N(t), \tag{67}$$

where $y(t)$ is column-wise vector of $y(t)$, $y(t-1)$, $\ldots$, $y(t-p)$ and matrix A looks the following way:

$$\begin{pmatrix} A_1 & A_2 & \cdots & A_{p-1} & A_p \\ I & 0_{n,n} & \cdots & 0_{n,n} & 0_{n,n} \\ 0_{n,n} & I & \cdots & 0_{n,n} & 0_{n,n} \\ \vdots & \vdots & \ddots & 0_{n,n} & 0_{n,n} \\ 0_{n,n} & 0_{n,n} & \cdots & I & 0_{n,n} \end{pmatrix}, \tag{68}$$

all matrices being $n \times n$. That allows to compute $y(t+1)$ as a column wise vector composed of $y(t+1)$, $y(t)$, $\ldots$, $y(t-p+1)$, where $y(t+1)$ is actual new point of a signal and the rest is previous p points, which are going to be used in the next iteration.

```
A = zeros(nChannels*order);
A(1:nChannels, :) = Amatrix;
A(nChannels+1:end, 1:(order-1)*nChannels) = eye((order-1)*nChannels);
signal = zeros([nChannels*order points]);
signal(:,1) = randn([nChannels*order 1]);
A = real(A);

for i=2:points
    n = randn([nChannels*order 1])-0.5;
    signal(:, i) = A*signal(:, i-1)+n;
end

signal = signal(1:nChannels, :);
```

Listing 3: Creating a signal

5.2 Computing brain connectivity estimators

5.2.1 Partial directed coherence

Function findPDC provides computed partial directed coherence for the input range of frequencies. Matrix for $A(z)$ is also part of the input parameters.

```
function pi = findPDC(Aofz, lower, higher)
   [order, ~] = size(Aofz);
   pi = [];
   for i = 1:(higher-lower+1)
      pitemp = Aofz(:,:,i);
      temp = Aofz(:,:,i);
```

```
    denom = sqrt(sum(abs(temp).^2, 1));
    for k = 1:order
       pitemp(k, :) = abs(pitemp(k, :))./denom;
    end;
    pi = cat(3, pi, pitemp);
end;
```

Function returns a 3D array of PDC matrices concatenated along the 3rd dimension.

5.2.2 Spectra and coherence

Function findCoherence computes auto- and cross-spectra and coherence from the given range of frequencies.

```
for i = 1:(higher-lower+1)
    Azinv = inv(Az(:,:,i));
    partSpectra = Azinv*C*transpose(conj(Azinv));
    spectra = cat(3, spectra, partSpectra);

    coherencePart = zeros(order);
    for k = 1:order
        for m = 1:order
            coherencePart(k,m) = abs(partSpectra(k,m)/...
                sqrt(partSpectra(k,k) * partSpectra(m,m)));
        end
    end
    coherence = cat(3, coherence, coherencePart);
end;
```

Output is two 3D matrices of spectra and coherence concatenated along the 3rd dimension.

5.3 AR fitting

For AR fitting there was used an algorithm presented by Schack et al. [10]. All that was needed was careful implementation. Crucial part of an algorithm

```
for i = order+1:signalLength
    Wn = [];
    for j = 1 : order
        Wn = cat(2, Wn, (signal(:, i - j)).');
    end
    tmp = Wn*C*(Wn.') + 1;
```

```
    aux = (Wn.')*Wn*C/tmp;

    C = C*(eye(signalDimension*order) - aux)/(1-forgettingFactor);
    K = Wn * C;
    Zn = signal(:, i)' - Wn*(Theta)';
    W1 = Zn'*Zn;
    Theta = Theta + (Zn') * K;
    Zn = signal(:, i)' - Wn*(Theta)';
    W2 = Zn'*Zn;
    forgettingFactor1 = 0.05;
    Sigmai = (1-forgettingFactor1)*Sigma(:, end-signalDimension+1:end) + ...
      (forgettingFactor1*0.5*(W1 + W2))';
    Sigma = cat(2, Sigma, Sigmai);
end
```

Listing 4: AR fitting by Schack et al.

The function takes a signal, desired order and forgetting factor as input parameters and computes Θ, which is $[A_1, A_2, \ldots, A_p]$, where p is desired order of the model. The function was tested on the artificial signals with known random seed and covariance matrix of the noise, but to ensure absence of human error, code provided by the thesis advisor was used for the actual computation.

6 Conclusion

During the work on this thesis I've studied an excessive amount of information, books and articles on brain functioning, linear mathematics and data analysis. I've learned a lot and deepened my knowledge in math and programming. I've got a glance of a new and exciting field, which I hope to continue with in the future with the goal of deepening our understanding of the human brain.

This thesis presented an overview of methods of estimating and quantifying connections among sources of electrical activity. The methods were tried on randomized simulations of electrical activity to determine their feasibility. This thesis, in a way, proved eligibility of using Independent Component Analysis for studying brain functional connectivity.

Selected methods were used on real EEG data and some functional connections were found. This work will serve as a basis for an article, which will may later be published.

Lenka Lavlinskaya

References

[1] Julie Onton, Marissa Westerfield, Jeanne Townsend, Scott Makeig, *Imaging human EEG dynamics using independent component analysis*, Neuroscience and Biobehavioral Revies 30 (2006) 808-822

[2] Roberta Grech, Tracey Cassar, Joseph Muscat, Kenneth P Camilleri, Simon G Fabri, Michalis Zervakis, Petros Xanthopoulos, Vangelis Sakkalis, Bart Vanrumste, *Review on solving the inverse problem in EEG source analysis*, Journal of NeuroEngineering and Rehabilitation, pp. 5-25

[3] Grosse-Wentrup M., *Understanding Brain Connectivity Patterns during Motor Imagery for Brain-Computer Interfacing*, Max Planck Institute for Biological Cybernetics

[4] Cardoso, J.-F., Laheld, B., *Equivariant adaptive source separation*, IEEE Transactions on Signal Processing 44, 3017–3030, 1996

[5] Bell, A.J., Sejnowski, T.J., *An information-maximization approach to blind separation and blind deconvolution*, Neural Computation 7, 1129–1159, 1995

[6] Hyvrinen, A., Karhunen, J., Oja, E., *Independent component analysis*, 2001, New York: J. Wiley, ISBN 0-471-22131-7

[7] Molgedey, L., Schuster, H.G., *Separation of a mixture of independent signals using time delayed correlations*, Physical Review Letters 72, 3634–3637, 1994

[8] V.S. Ramachandran, *The Tell-Tale Brain: A Neuroscientists's Quest for What Makes Us Human*, W. W. Norton & Company, ISBN 978-0-393-07782-7

[9] Eva Möller, Bärbel Schack, Matthias Arnold, Herbert Witte, *Instantaneous multivariate EEG coherence analysis by means of adaptive high-dimensional autoregressive models*, Journal of neuroscience methods, vol. 105, pp. 143-158

[10] Wolfram Hesse, Eva Möller, Matthias Arnold, Bärbel Schack, *The use of time-variant EEG Granger causality for inspecting directed interdependencies of neural assemblies*, Journal of neuroscience methods, vol. 124, pp. 27-44

[11] P.D. Bobrov, A.V. Korshakov, V.Yu. Roschin, A.A. Frolov, *Bayesian Classifier for Brain-Computer Interface Based on Mental Representation of Movements*, Journal of Higher Neural Activity, 2012, 62, pp. 89-99

[12] Maciej Kamiński, Mingzhou Ding, Wilson A. Truccolo, Steven L. Bressler, *Evaluating casual relations in neural systems: Granger causality, directed transfer function and statistical assessment of significance*, Biol Cybern, 2001, 85, pp. 145-157

[13] Pavel Bobrov, Alexander Frolov, Charles Cantor, Irina Fedulova, Mikhail Bakhnyan, Alexander Zhavoronkov, *Brain-Computer Interface Based on Generation of Visual Images*, PLoS ONE, June 2011, vol. 6

[14] Alexander Frolov, Dušan Húsek, Pavel Bobrov, *Comparison of four classification methods for brain-computer interface*, Neural Network World, 2011, pp. 21-37

[15] C.W.J. Granger, *Investigating Casual Relations by Econometric Models and Cross-spectral Methods*, Econometrica, 37 (3), pp. 424–438

[16] Wolfgang Klimesch, *EEG alpha and theta oscillations reflect cognitive and memory performance: a review and analysis*, Brain Research Review, 1999, 29, pp. 169-195

[17] A.V. Kurgansky, *Some Methodological Issues of Studying Cortico-Cortical Functional Connectivity with Vector Autoregressive Model of Multichannel EEG*, Journal of Higher Neural Activity, 2010, pp. 630-649

[18] Niedermeyer E. and da Silva F.L., *Electroencephalography: Basic Principles, Clinical Applications, and Related Fields*, Lippincot Williams & Wilkins, ISBN 0-7817-5126-8, 2004

[19] Romain Grandchamp, Claire Braboszcz, Scott Makeig, Arnaud Delorme, *Stability of ICA decomposition across within-subject EEG datasets*, 34th Annual International Conference of the IEEE EMBS, San Diego California USA, 28 August - 1 September, 2012

[20] Frolov A., Husek D., Bobrov P. et al., *Sources of EEG activity most relevant to performance of brain computer interface based on motor imagery*, Neural Network World, 2012, V. 22, P. 21

[21] Frolov A., Husek D., Bobrov P., Mokienko O., Tintěra J., *Sources of Electrical Brain Activity Most Relevant to Performance of Brain-Computer Interface Based on Motor Imagery*, In Brain-Computer Interface Systems - Recent Progress and Future Prospects, Rijeka, InTech, 2013, s. 175-193, ISBN 978-953-51-1134-4

[22] Baccala L. A., Sameshima K., *Partial directed coherence: A new conception in neural structure determination*, Biol Cybern, 2011, 84 (6), pp. 463–474

[23] Kaminski M., Blinowska K. J., *A new method of the description of the information flow in brain structures*, Biol Cybern, 1991, 65 (3), pp. 203–210

[24] Korzeniewska A., Mańczak M., Kaminski M., Blinowska K. J., Kasicki S. *Determination of information flow direction among brain structures by a modified Directed Transfer Function method (dDTF)*, J Neurosci Methods, 2003, 125 (1–2), pp. 195–207

[25] Caines P.E., Chan C.W., *Feedback between stationary stochastic processes*, IEEE Trans Autom Control 20, 1975, pp. 498-508

[26] Geweke J., *Measurement of linear dependence and feedback between multiple time series*, J Am Stat Assoc, 1982, 77, pp. 304-313

[27] Marple S.L., *Digital spectral analysis with applications*, Prentice Hall, 1987, ISBN-13 978-0132141499

[28] Schneider T., Neumaier A., *ARfit – A Matlab package for the estimation of parameters and eigenmodes of multivariate autoregressive models*, Algorithm 808, ACM Trans. Math. Software., 2001, 27(1), pp. 58–65

[29] Saito Y., Harashima H., *Tracking of information within multichannel EEG record*, Recent advances in EEG and EMG data processing, Elsevier, Amsterdam, 1981, pp 133-146

[30] Wang G., Takigawa M., *Directed coherence as a measure of interhemispheric correlation of EEG*, Int J Psychophysiol, 1992, 13, pp. 119-128

[31] Bernasconi C., König P., *On the directionality of cortical in- teractions studied by structural analysis of electrophysiological recordings*, Biol Cybern, 1999, 81, pp. 199 - 210

A Contents of the attached disc

On the disc attached to the printout are the following directories and files:

ext Files used in computations obtained from the thesis advisor.

functions Original files used in computations.

workscripts Miscellaneous related files.